

## A numerical investigation and geological discussion of the relationship between folding, kinking and faulting

J-P. LATHAM\*

Department of Geology, Imperial College, London, SW7 2BP, U.K.

(Received 8 March 1984; accepted in revised form 1 October 1984)

**Abstract**—The layer-parallel compression of a regular bilaminate consisting of layers with materials described by an incompressible power-law elastic model is considered. The average mechanical properties of this idealised multilayer are then represented by those of an equivalent anisotropic continuum with internal resistance to bending. Changes in material properties that accompany uniform finite shortening are accounted for. Interpretation of the internal instability analysis for such a continuum, introduced in the companion paper involves the use of a spectrum which at a given level of strain, scans all directions within the continuum for relative susceptibility to a heterogeneous simple shearing instability.

Estimates of nonlinear material properties from reported experiments on the behaviour of various rocks in the time-independent deformation regime, and geometric parameters such as the volume fraction of each material and the number of confined layers are considered. The shapes of the resulting spectra may be used to predict natural conditions that will favour the initiation of repetitive buckle folds or more localized disturbances such as kink-bands and faults. Results suggest that for typical properties of sedimentary multilayers, kinking is strongly favoured over repetitive buckling where the weaker material occupies only a very small volume fraction of the multilayer. The effect of significant imperfections leading to slippage between layers is discussed.

Finally, a simple classification of structure genesis is proposed in which the mechanical relationships between apparently diverse structures is illustrated.

### INTRODUCTION

WHETHER multilayers of sedimentary rocks will fault or fold when subjected to layer-parallel shortening was investigated by Johnson (1980) using a theory for elastic-plastic strain-hardening materials. The conclusions that Johnson arrived at follow from an analysis which considers one of the most common situations in natural sedimentary multilayers. That is, the layer-parallel compression of (an unspecified number of) competent layers, such as sandstones, siltstones or limestones, in weak contact with each other, for example due to high pore-fluid pressure (Price 1975) and embedded within a less competent medium such as shale. His analysis shows that for the properties of a particular suite of sedimentary rocks, obtained from laboratory data, the multilayer will fold rather than produce reverse faults provided there are at least two or three effectively frictionless horizons separating the competent units.

The purpose of this paper is to use a completely different approach to what is a comparable multilayer problem. The approach followed here uses an analysis for internal instability in multilayers that incorporates the effects of bending resistance and nonlinear material properties presented in a companion paper (Latham 1985). This analysis takes into account the amount of uniform shortening and allows the layer properties to change with deformation (as does Johnson's (1980) analysis). What the analysis loses in generality by the restricting specification of rigid confinement of the multilayer, it gains by the diversity of geologically meaningful

material behaviour that can be treated. As explained in detail in the companion paper, the analysis uses the well tried approach introduced by Biot (1964, 1965, 1965a, 1965b, 1965c) for linear viscous, elastic and viscoelastic multilayers. A regular and adhering bilaminar composite is analysed in terms of the response of an equivalent homogeneous continuum with average anisotropic properties. Sedimentary multilayers where stiff and weak layers alternate regularly are the rule of nature rather than the exception, making the bilaminate an extremely relevant idealized model for investigation.

The geological application of Biot's (1965) theory of internal instability presented by Cobbold *et al.* (1971) made only minimal reference to the possibility of faulting and generally Biot's theory has been regarded as having nothing to contribute to the study of faulting mechanisms. The analysis of Johnson (1980) indicates otherwise and this important connection is discussed in the final section of this paper.

The numerical investigation of geologically meaningful multilayer parameters uses a new spectrum technique which is introduced below.

### INSTABILITY PARAMETER ( $\zeta$ ) SPECTRA

One common criticism of Biot's (1965, pp. 192–204) discussion of internal instability is that he holds fixed the moduli  $M$  and  $L$ . Whereas for linear materials, this may not lead to inconsistencies in the interpretations of instability solutions, for nonlinear materials it is essential to include the dependence of  $M$ ,  $L$  and  $P$  and thus the instability itself upon the finite uniform strain. To give a clearer illustration of the internal instability condition for the power law I.M.M. (Idealized Multilayer Model,

\* Present address: Department of Geography and Earth Science, Queen Mary College, London E1 4NS, U.K.

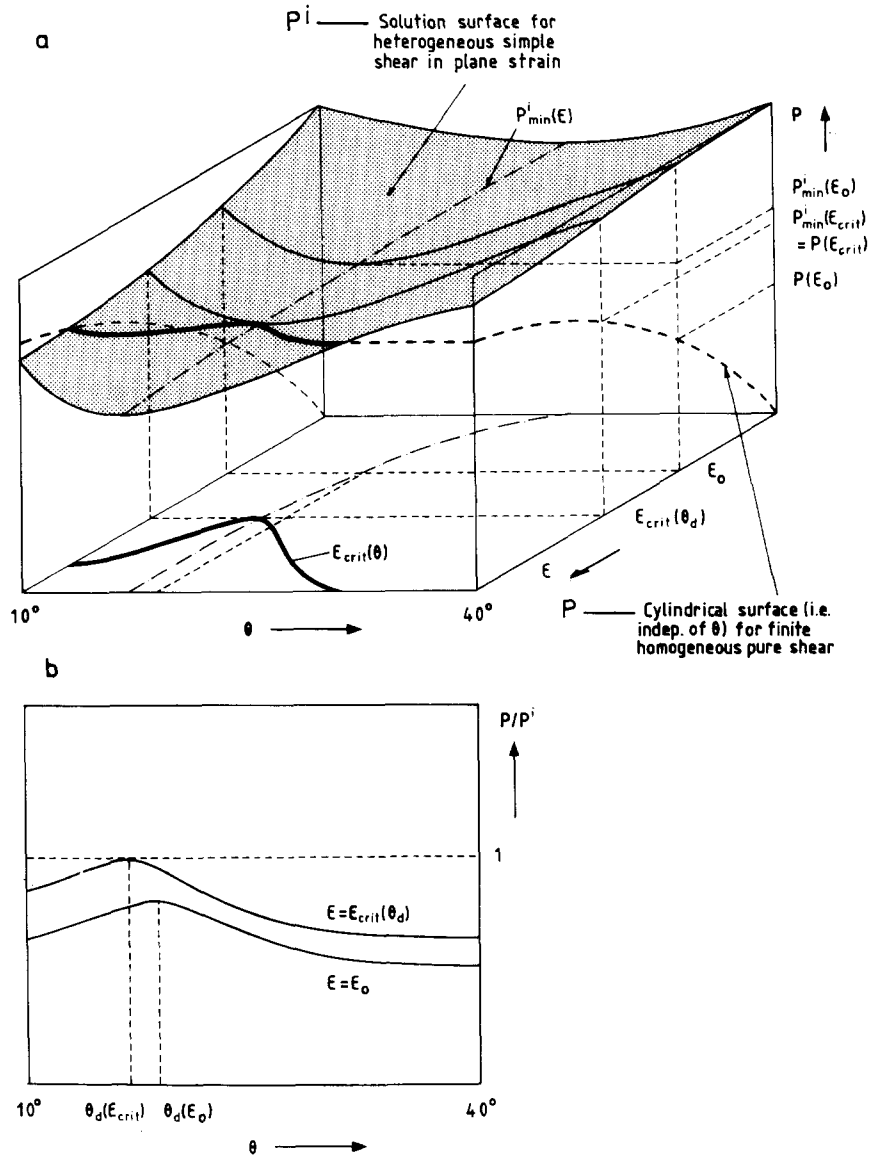


Fig. 1. (a)  $P$ - $\epsilon$ - $\theta$  diagram showing a portion of the plane-strain internal instability solution surface for heterogeneous simple shear along characteristic directions  $\theta$  in time-independent anisotropic media. (b) A portion of the  $\zeta$ -spectrum obtained by dividing the stress required for instability  $P^i$  by the applied stress  $P$  appropriate for a chosen amount of uniform strain. See text for discussion.

see Latham 1985), a three dimensional  $P$ - $\epsilon$ - $\theta$  plot is helpful (Fig. 1) (cf. the two-dimensional  $P$ - $\xi$  plots of Biot 1965, pp. 196-200).

*Explanation of Fig. 1*

The three-dimensional illustration follows from a variational analysis of internal instability (Biot 1965, p. 203, 1967, p. 407). If we examine equation (29) of Latham (1985)

$$P = L \left\{ 1 + \frac{a}{\xi^2} + 2 \frac{(2M - L)}{L} \xi^2 + \xi^4 \right\}$$

and set the R.H.S. equal to  $P^i$  (the  $i$  chosen to signify instability level association with specific real characteristics), then when the L.H.S.,  $P$ , is greater than  $P^i$ , more strain energy is available in the uniform initial compression than is required to initiate an internal instability;

that is, real solutions describing heterogeneous simple shear in directions  $\pm\theta$  become available. Therefore, for any given layer-parallel shortening strain  $\epsilon$  and direction  $\theta$ , ( $= \tan^{-1} \xi$ ) the relationship between  $P$  and  $P^i$  is crucial to the stability condition for shear in that direction.

The differential stress  $P$ , (Latham 1985 eq. 19) is a function of  $\epsilon$ , the material properties and the proportions of each material;  $P^i$  is a more complex function of  $\epsilon$ ,  $\theta$  (or  $\xi$ ),  $M$ ,  $L$  and  $a$ . For an arbitrary choice of I.M.M. constants (i.e.  $k_1/k_2$ ,  $m_1$ ,  $m_2$ ,  $\alpha_1$ ,  $H$ ), Fig. 1 shows a typical  $P$ - $\epsilon$ - $\theta$  plot over the range  $10^\circ < \theta < 40^\circ$ . The functions  $P$  and  $P^i$  are represented as surfaces where  $P$  is cylindrical about the axis.

Consider now what happens to the hypothetical I.M.M. in Fig. 1 as an increasing differential stress forces the multilayer to shorten (uniformly to begin with). At a strain  $\epsilon_0$ ,  $P/P^i$  is  $< 1$  for all directions  $\theta$  and stability

prevails. With further shortening at  $\epsilon = \epsilon_{\text{crit}}(\theta_d)$  the two surfaces representing  $P$  and  $P^i$  intersect for the first time (i.e. at the lowest level of strain along the line of intersection of the two surfaces). This point of intersection is where  $\zeta (= P/P^i) = 1$ . This occurs at the critical strain  $\epsilon_{\text{crit}}(\theta_d)$  for which there exists a single pair of characteristics  $\pm(\theta_d)$  along which instability can propagate from even the smallest of imperfections in the multilayer or anisotropic continuum.

Figure 1(b) illustrates a portion of the  $\zeta$ -spectrum in the form in which theoretical results of specific I.M.M. examples are illustrated in Figs. 2 and 3. The  $\zeta$ -spectra are generated at different levels of strain from a determination of the relative heights of the two surfaces shown in the  $P$ - $\epsilon$ - $\theta$  diagram (i.e. across the appropriate constant strain sections of the diagram, see Fig. 1a).

At this point, it may be useful to remind the reader of Biot's two end-members of internal instability. The instability is a heterogeneous simple shearing along characteristic directions  $\theta_d$ . For first kind end-member behaviour,  $\theta_d \approx 0^\circ$  and an internal buckling pattern develops. For second kind end-member behaviour,  $\theta_d \approx 45^\circ$  and an oblique localized shearing propagates. For the hypothetical case shown in Fig. 1, the instability develops with  $\theta_d \approx 17^\circ$  and is likely to be one of hybrid form.

The following points of detail should be noted. If boundary conditions are such that the dimensions of the rectangular domain of material are specified so that the layers do not extend infinitely in the  $x$ -direction, then first-kind instability may be delayed to shortening strains greater than  $\epsilon_{\text{crit}}(\theta_d)$ . However, shear localization associated with second-kind instability cannot generally be suppressed by this kind of kinematic control of the boundary dimensions (Rice 1976). Once internal instability is incipient (signified by a first-order bifurcation in the equilibrium path upon exit from the E regime in Fig. 7 of the companion paper), the theoretical relationship for  $\epsilon > \epsilon_{\text{crit}}(\theta_d)$  generally becomes meaningless because the theory cannot account for the fact that some parts of the multilayer will be loading while others are unloading.

#### Method of plotting $\zeta$ -spectra

Defining  $\zeta$  as the ratio  $P/P^i$ , the  $\zeta$ -spectrum is plotted for a given set of I.M.M. constants simply by scanning  $\zeta$  for all values of  $\theta$ , 0 to  $90^\circ$  in  $1^\circ$  intervals, at any chosen level of strain. Using a method of trial and error, approximate solutions (sufficiently accurate for the needs of the present investigation) for the critical strain  $\epsilon_{\text{crit}}(\theta_d)$  at which dominant characteristics develop, are readily obtainable with interactive use of computer facilities. Note (see Fig. 1a) that solving for  $\epsilon_{\text{crit}}(\theta)$ , that is where  $\zeta = 1$  for each value of  $\theta$ , is not so practicable and consequently it is the  $\zeta$ -spectral method of examining instability which is pursued below.

#### Spectrum shapes

With so many multilayer variables affecting stability,

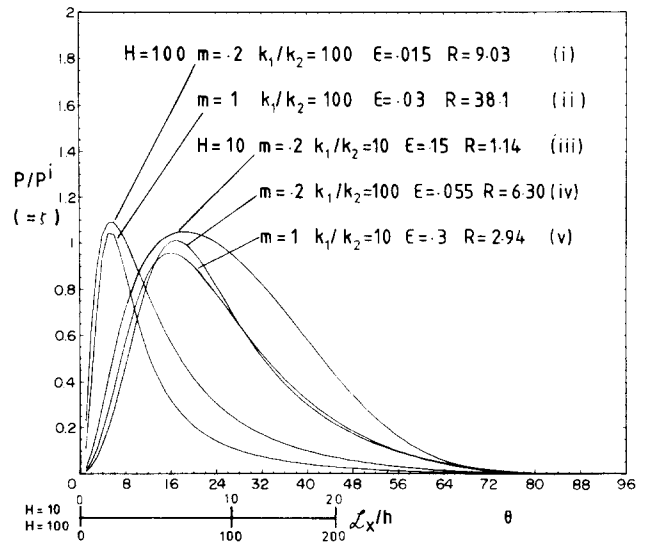


Fig. 2.  $\zeta$ -spectra for five different multilayers with high intrinsic anisotropy. For homogeneous pure shear, the differential stress  $P$  in each layer is governed by a power law of the form  $P = ke^m$ , see Fig. 4. The hardening exponent  $m$  is identical in both layers within each multilayer considered, i.e.  $m = m_1 = m_2$ . The ratio  $k_1/k_2 (=k_r)$  is the ratio of the linear stiffness constants for each layer (equivalent to the competence contrast) and  $H$  is the number of confined layers.  $R$ , defined in the companion paper, is greater than one for each multilayer and therefore signifies that buckling is the preferred end member instability. The normalized wavelength of internal buckles,  $L_x/h$ , is given as an alternative measure on the abscissa. Note that the logarithmic strain  $\epsilon$  given in the plots is only an approximate determination for the critical strain  $\epsilon_{\text{crit}}(\theta_d)$  at which the multilayer first becomes critically unstable. The fractional thickness,  $\alpha_1 = 0.5$  in each multilayer.

it is not practical to present a systematic illustration of the effect of each variable on stability conditions. Nevertheless, a selection of  $\zeta$ -spectra for which  $\epsilon \approx \epsilon_{\text{crit}}(\theta_d)$  are shown in Fig. 2. Each of the five multilayers considered reach a critical strain with  $R > 1$ , where  $R = (M/L)/(0.5 + 0.75a^{1/3})$  (Latham 1985, eq. (43)). This is because all these multilayers have a high contribution from *intrinsic anisotropy* as the instability condition is reached. Internal buckling develops in all cases but noticeably at much lower strains in (i), (ii) and (iv) in Fig. 2. The typical shape of the  $\zeta$ -spectrum for first-kind instability end member (with the total number of confined layers,  $H$ , between 10 and 1000) is for  $\zeta$  to increase smoothly from 0 at  $\theta = 0^\circ$  to a peak at  $3^\circ < \theta < 20^\circ$  and to fall smoothly to insignificant values for  $\theta = 45^\circ$ .

The effect of having fewer confined layers (lower  $H$ ) is to broaden and shift the peak in the spectrum; the onset of buckling is retarded and folds of longer wavelength are produced. For multilayers with a large number of layers (as  $H \rightarrow \infty$ ,  $a \rightarrow 0$ , see Latham 1985) the embryonic folds take on a more ideal similar geometry since  $\theta \rightarrow 0$  also.

Figure 3 gives the  $\zeta$ -spectra for two multilayers (iii) and (iv) and two isotropic media (i) and (ii) all four having highly nonlinear (low  $m$ ) properties. Induced incremental anisotropy is therefore likely to play an important role at instability for these examples. The typical shape of the  $\zeta$ -spectrum for the second-kind instability end member is for marked peaks to appear

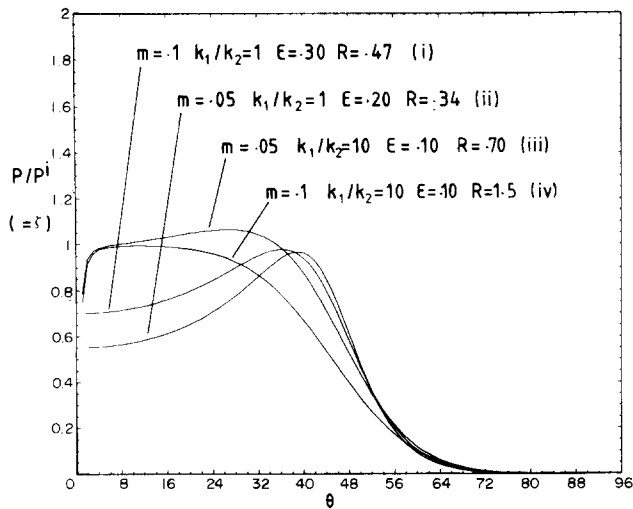


Fig. 3.  $\zeta$ -spectra for two multilayers with equal layer thicknesses ( $\alpha_1 = 0.5$ ) and 100 confined layers ( $H = 100$ ) and for two intrinsically isotropic blocks of material. A high anisotropy is induced in each case and  $m = m_1 = m_2$ . Note the flat top to curves (iii) and (iv). see text.

between 35 and 45° (see (i) and (ii) in Fig. 3), but where  $\zeta$  does not rise monotonically from 0 at  $\theta = 0^\circ$  to its peak value. The isotropic examples are special cases of the I.M.M. and have been the subject of detailed shear-band analysis by Hutchinson & Tvergaard (1981). Using an identical power-law constitutive model, they showed that the critical strain condition for the dominant characteristic direction  $\theta_d$ , that is, the first formed shear band, is

$$\epsilon_{\text{crit}} = [mq(\epsilon_{\text{crit}}) - m]^{1/2}$$

where

$$q(\epsilon_{\text{crit}}) = 2\epsilon_{\text{crit}} \coth(2\epsilon_{\text{crit}})$$

and that the shear-band angle and critical finite stretch  $\lambda_{\text{crit}}$  are simply related by

$$\tan \theta_d = e^{-\epsilon_{\text{crit}}} = \lambda_{\text{crit}}.$$

Confirmation of these relationships is given by the  $\zeta$ -spectra of (i) and (ii) (Fig. 3). If  $\theta_1$  is the orientation of the material line in the undeformed state which later becomes the shear band, Hutchinson & Tvergaard (op. cit.) also show that the relationship can be simply expressed as

$$\theta_1 + \theta_d = \pi/2.$$

The shapes of the  $\zeta$ -spectra for (iii) and (iv) (Fig. 3) differ markedly from the others considered so far in that  $\zeta \cong 1$  over a range of about 30°, giving the significant result that the spectra have flat tops. The interpretation offered is that the selectivity of the dominant characteristic is poor and that the instability is in a sense an almost perfect hybrid between internal buckling and shear localization for these multilayers (a suggestion supported by the value of  $R$ ). Both (iii) and (iv), with  $k_1/k_2 = 10$ , reach critical strains at approximately the same value; however the values of  $R$  and the shape of the  $\zeta$ -spectra indicate that in (iv), internal buckling is preferred ( $\theta_d \approx 11^\circ$ , or alternatively, the buckling wavelength to average layer thickness ratio,  $\mathcal{L}_x/h \approx 39$ )

and in (iii), localized shearing ( $\theta_d \approx 27^\circ$ ) can be expected to prevail because of the more nonlinear properties.

So far, the  $\zeta$ -spectra considered have been chosen to illustrate a range of mathematical possibilities of the analysis. To go further and draw out the geological implications of any  $\zeta$ -spectra results, it is necessary to make hypotheses about the interpretation of different  $\zeta$ -spectrum shapes. For example, even without recourse to finite element or post-bifurcation analysis, it seems reasonable to suggest that the initial post-bifurcation deformation generated in multilayer (iii) of Fig. 3, would express physically the hybrid nature of the instability as suggested by the  $\zeta$ -spectrum. For this multilayer the tendency of the intrinsic anisotropic properties is to produce a flexing of the layering while at the same time, the stress-induced effect of material nonlinearity is to encourage a deformation which allows for the propagation of certain discontinuities in displacements and displacement derivatives. It is therefore proposed that *conjugate kink bands* are more likely as finite structures than discrete shear fractures for this idealized multilayer (iii).

## GEOLOGICAL CONSIDERATIONS

### Interlayer slip

The analyses of Johnson and the present author will first be compared. Johnson (1977, p. 356, 1980) considered two different nonlinear constitutive models in folding analyses. His conclusions regarding multilayer behaviour in sedimentary rocks appear to have been drawn from theoretical examinations of the behaviour of single layers in layer-parallel compression. The boundary conditions chosen were those appropriate when identical layers are in an embedded multilayer stack with either perfect slip or perfect adherence between them. The analysis in the present paper considers the multilayers' average mechanical response for repeated alternations of different materials making up the multilayer [as does earlier work presented by Johnson (1977, Chapter 6) but for linear elastic multilayers]. It is therefore not directly applicable to the geologically important case, discussed by Johnson (1980), of cohesion loss or slip between identical competent layers.

Nevertheless, as an approximation and applying the present analysis, it is useful to consider the effect of a local loss of interlayer strength as being equivalent to that of a generalized weakness imperfection. The  $\zeta$ -spectrum shape at strains below that which is critical for the perfect multilayer is then likely to be meaningful for many real (i.e. imperfectly bonded) multilayers. Such sub-critical spectra, it is suggested, can indicate a preference for characteristics associated with the early development of folding, faulting or kinking instabilities. In some cases, it may be possible with the sub-critical  $\zeta$ -spectrum to predict the unstable response to a local development of high pore fluid pressure or even to a significant initial perturbation in the layering, either of which could trigger early interlayer slip.

*Material properties*

The analysis presented in the companion paper and developed further in this paper is for time-independent material properties and is therefore aimed at structures in sedimentary rocks in the appropriate deformation environment, i.e. at high levels in the Earth's crust where cataclastic, intracrystalline glide and twinning deformations are dominant over diffusion and mass transfer processes. There are two major assumptions in the theory concerning material properties, that restrict its application in the prediction of structure initiation in sedimentary multilayers.

(1) The assumption that the material continues to deform by the prescribed power-law constants regardless of the state of strain. This does not allow for a realistic level of strain for imminent failure or for zero and negative hardening moduli. The problem could be overcome by using an elastic-plastic constitutive model fitted from experimental data where for the strain at failure the hardening modulus approaches zero (see Johnson 1980).

(2) The assumption of incompressibility. Significant porosity in sedimentary rocks, which is intimately linked with compressibility and pore fluid pressure effects, can rarely be ruled out from upper crustal sedimentary sequences. The effects of dilatant and pressure sensitive (e.g. frictional) behaviour upon the localization of deformation and the orientation of the bands produced was investigated by Rudnicki & Rice (1975) and more recently placed in the context of geological faulting by Aydin & Johnson (1983). Because of the complexities involved, theoretical consideration of compressibility and other more realistic features of rock deformation in the upper crust are regarded as valuable but not essential refinements, to the relatively simple numerical analysis presented below.

Finally, for the numerical analysis, what values of  $k$  and  $m$  are most appropriate for the material properties of a geologically meaningful multilayer model?

Four sets of values of the power-law material constants  $m$  and  $k$  have been proposed for four theoretical rock types A, B, C, and D. Their corresponding stress/strain curves are shown in Fig. 4 and may be compared with available laboratory data (most favourably for confining pressures of ~2 kb) using the stress scale in the figure multiplied by a factor between 1 and 5.

Johnson (1977, p. 364) has tabulated power-law constants from a selection of triaxial compression test data on sandstones, siltstones, limestones and shales at 1 and 2 kb confining pressure. Values obtained from the table for 2 kb confining pressure are:  $m = 0.65$ ,  $k = 16.6$  kb for Repetto Siltstone;  $m = 0.21$ ,  $k = 8.15$  kb for Barnes Sandstone and  $m = 0.32$ ,  $k = 5.08$  kb for Green River Shale. Note that the relationship

$$k = 2 \left( \frac{2}{\sqrt{3}} \right)^{m+1} (2g)^m$$

is used to convert the triaxial data constant,  $2g$ , used by Johnson to the constant  $k$  for pure shear.

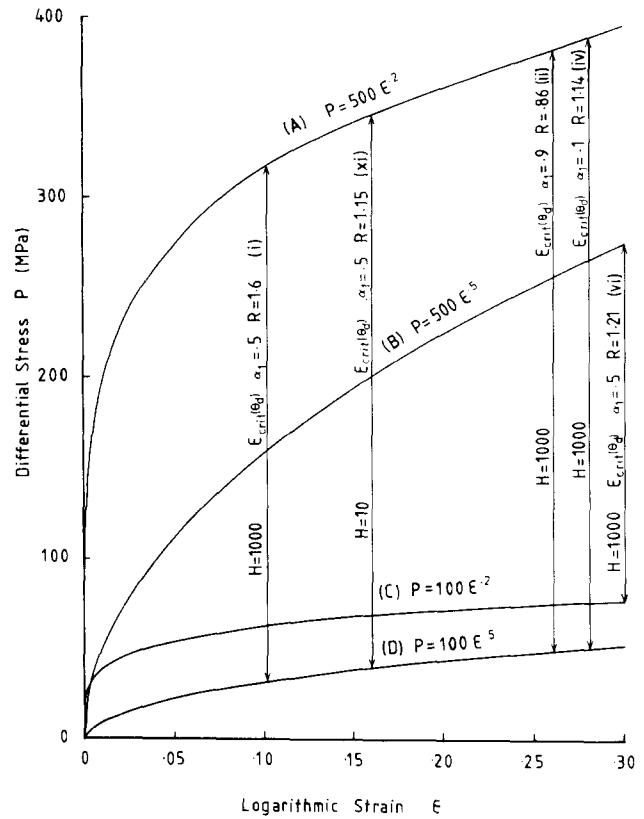


Fig. 4. Hypothetical stress/strain curves for four different power-law materials ( $P = k\epsilon^m$ ) deformed in a uniform pure shear. The stress scale (100MPa = 1 kb) has been chosen to facilitate a comparison with experimental laboratory data obtained for rocks. The diagram also shows the predicted critical strains for various I.M.M.'s that are discussed in Figs. 5-9. See text for discussion.

For multilayers of rocks A and D, or B and C, we shall therefore be considering the value of  $k_1/k_2 = 5$ , with  $m_1 = 0.2$ ,  $m_2 = 0.5$  and also  $m_1 = 0.5$ ,  $m_2 = 0.2$  to be geologically significant. Furthermore, in a multilayer, the absolute  $k$  values are not critical. It is the ratio  $k_r$  ( $= k_1/k_2$ ) that affects the stability.

**RESULTS**

As an interpretative aid to the examination of selected spectra, the meaning of  $R$  should perhaps be recalled. The parameter  $R$  is closely related to the degree of incremental anisotropy and includes the effect of resistance to bending. It provides a precise measure of what proportion of end-member features to expect from a range of possible low-amplitude rock structures, on the theoretical basis of how far into the fields of first- or second-kind instability a particular idealized and geologically relevant (coherent) multilayer is at a given level of strain.  $R$  values considerably above 1 are associated with first-kind instability and  $R$  values considerably below 1 are associated with second-kind instability. Instability occurring in multilayers when  $R \approx 1$  (between 0.85 and 1.18) will initially reflect their affinity with both fields of instability and it seems reasonable to suggest that flexing will combine with shear localization during early stages in the developing structure.

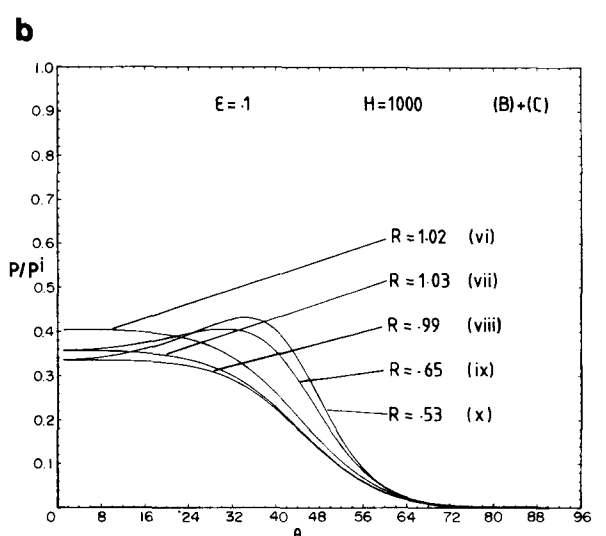
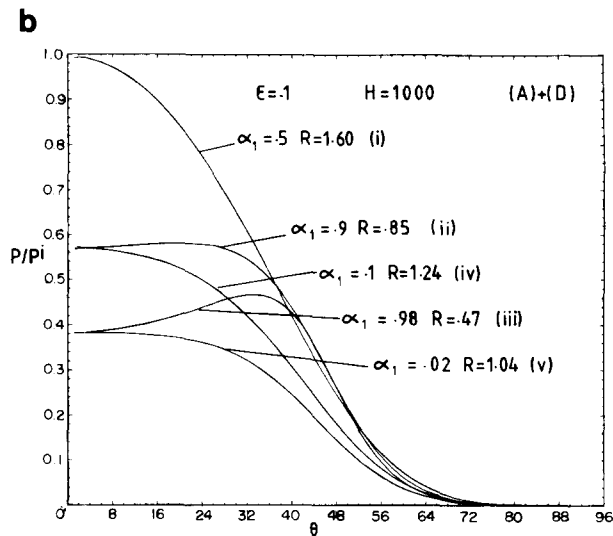
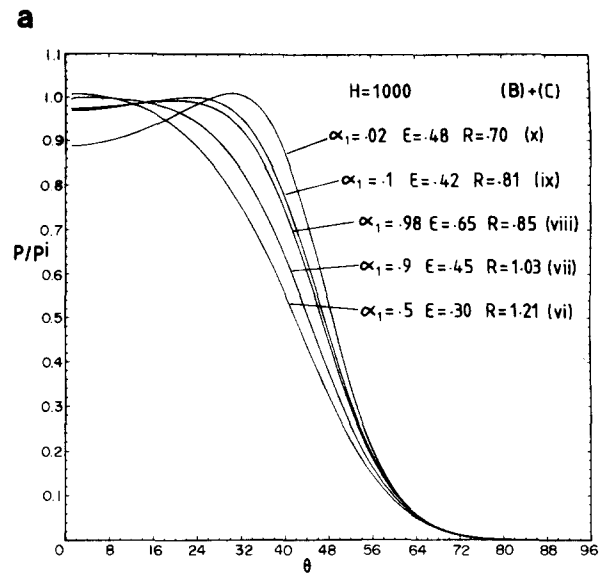
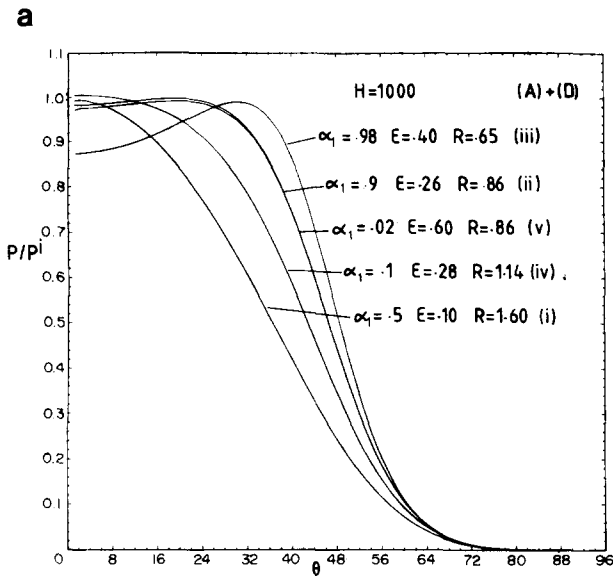


Fig. 5. The influence of different layer thickness ratios,  $\alpha_1$ , on the  $\zeta$ -spectra for power-law elastic multilayers illustrated in Fig. 9. The material properties of the alternating layers are given by curves (A) and (D) in Fig. 4. The I.M.M. parameters are  $m_1 = 0.2, m_2 = 0.5, k_1/k_2 = 5$  and there are 1000 confined layers ( $H = 1000$ ). (a) Spectra for  $\epsilon = \epsilon_{crit}(\theta_d)$ , the critical strain predicted for instability in the perfect multilayer. (b) Spectra for  $\epsilon = 0.1$ . The form of these spectra is used as a basis for predictions of the unstable response of the multilayers assuming that an imperfection locally triggers interlayer sliding at a bulk strain of  $\epsilon = 0.1$ .

Fig. 6. As for Fig. 5, the differences being that the material properties of the alternating layers are given by curves (B) and (C) rather than (A) and (D) in Fig. 4.

One further aspect of the multilayer models investigated which has not been mentioned is the possibility of single-layer buckling within the multilayer. Johnson (1977, p. 361) gives theoretical expressions for the critical stress for single-layer buckling of an embedded power-law elastic layer and also for the wavelength/thickness ratio in terms of the initial layer-parallel strain and the four material constants of the layer and matrix. However, he concludes from his more recent analysis of the same problem assuming elastic-plastic strain hardening material (Johnson 1980, p. 275), that the layer or medium will fault before the initial perturbation becomes amplified significantly. In the power-law multilayer model a consideration of single-layer buckling

becomes important when the stiffer layer occupies a sufficiently small fraction of the multilayer. In this case, faulting or buckling of individual layers may occur at strains well below the critical strain for the entire multilayer. Average anisotropic properties cannot represent the unstable behaviour of these multilayers nor that for highly irregular ones. Propagation of failure planes and the possible subsequent development of bedding plane thrusts is a subject beyond the scope of this paper.

The spectra plotted in Figs. 5 and 7 are multilayers with 1000 and 10 confined layers, respectively ( $H = 1000$  and 10). The spectra in both figures are for multilayers of materials A alternating with D (see Fig. 4). Figure 6 considers  $H = 1000$  with B and C, a more stable combination than A and D.

*Unequal layer thicknesses*

By varying  $\alpha_1$ , the effect of different proportions of one material making up the multilayer can be examined

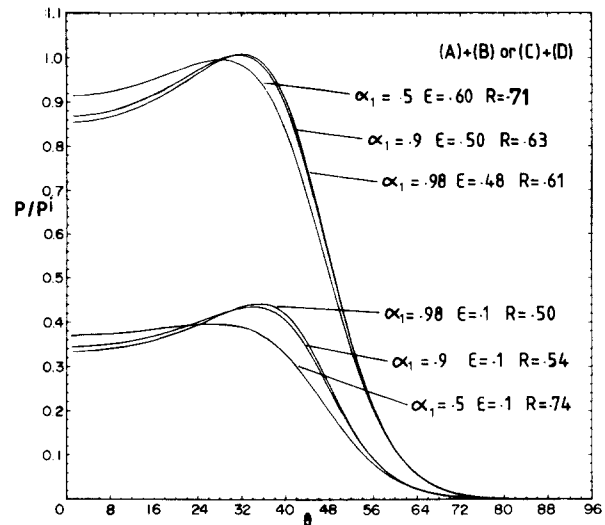
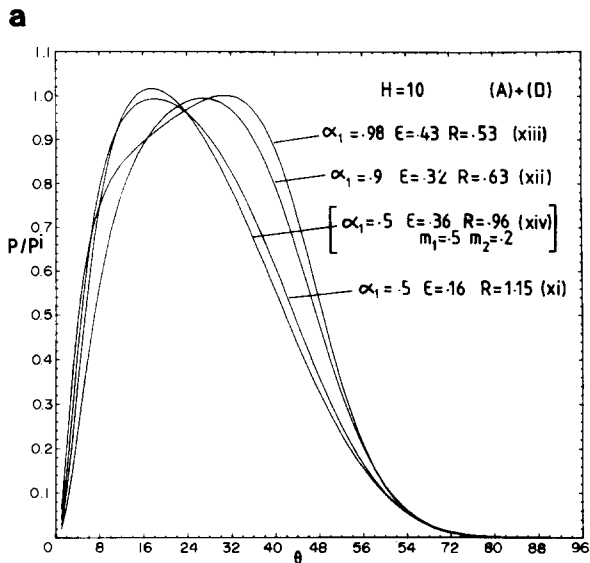


Fig. 8. Spectra for multilayers with  $k_1/k_2 = 1$ ,  $m_1 = 0.2$ ,  $m_2 = 0.5$  and 1000 confined layers.

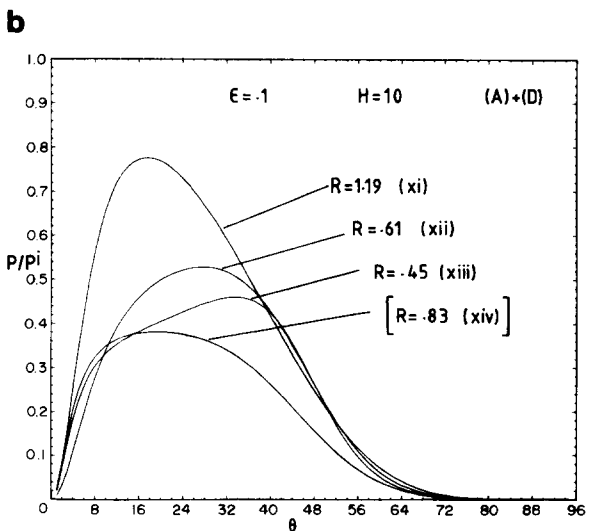


Fig. 7. As for Fig. 5, but with only 10 confined layers ( $H = 10$ ).

(for example A in Figs. 5 and 7). It is found that the value of  $\alpha_1$  has a profound effect on conditions of instability at the critical strain. For example, compare the spectra of Fig. 5(a) where the proportion of material A is varied from 2 to 98% of the whole multilayer. It can be seen that when  $\alpha_1 = 0.5$ , a well developed peak associated with first-kind instability has developed at  $\epsilon_{crit}(\theta_d) = 0.1$ . When  $\alpha_1 = 0.98$ ,  $\epsilon_{crit}(\theta_d) = 0.4$ ,  $\theta_d = 32^\circ$  and the  $\zeta$ -spectrum is associated with second-kind instability.

*Low initial competence contrast*

When both layers have the same  $k$  value (Fig. 8) the ideal multilayers (A and B, or C and D) are generally more stable and, of the multilayers examined, these are the least likely to buckle. The values of  $R$  are well below 1 in all cases and the spectra suggest that oblique shear localization should occur.

*Significant imperfections*

To take the subject of a physical interpretation of the analysis one step further, it is necessary to acknowledge the likely effect that imperfections, such as those mentioned in connection with interlayer slip, will have on predictions of instability based on incremental theory for perfect multilayers. The shape of the  $\zeta$ -spectra for  $\epsilon < \epsilon_{crit}(\theta_d)$  indicates the preferred orientation and degree of localization of amplifying perturbations on the assumption that at a given level of sub-critical strain for which the instability parameter spectrum is plotted, the imperfection is sufficient to trigger the propagation of a disturbance. To illustrate the geological results for imperfect multilayers, an arbitrary value of  $\epsilon = 0.1$  has been chosen as the destabilizing strain. The physical interpretations of the theoretical data examined in Figs. 4-8 are presented in Fig. 9 and discussed below.

For conditions in the multilayer where interfacial slip is triggered locally at a geometric imperfection, the theory predicts that two extreme kinds of unstable behaviour are possible and typical of two extreme types of multilayer.

(1) The intrinsic anisotropy is high and the average non-linearity of the material properties is low (e.g. large  $k_1/k_2$ ,  $m_1 \approx m_2 \approx 1$ ,  $\alpha_1 \approx 0.5$ ). The characteristic directions that offer least resistance to the average applied forces, are practically normal to the compression direction provided the multilayer offers little resistance to bending.

(2) The intrinsic anisotropy is low and the average non-linearity of the material properties is high leading to high induced anisotropy (e.g. low or moderate  $k_1/k_2$ ,  $m_1 \approx m_2 \approx 0.1$ ,  $\alpha_1 \approx 0.9$ ). The characteristic directions that are preferred are oblique (usually  $>30^\circ$ ) to the layer normal and the resulting structures are more localized than those in the first type of multilayer.

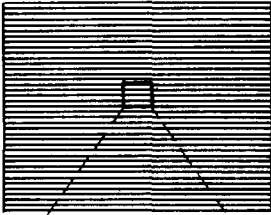




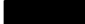


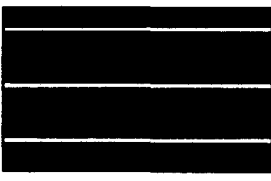

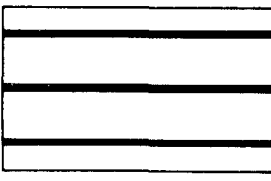
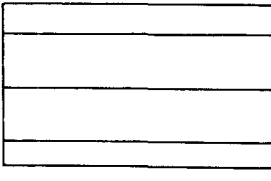
	<p>Interpretation based on <math>\zeta</math> spectra, see Fig.5</p> <p>  (D)   (A)                 </p> <p>For material properties of (A), (B), (C), (D) see Fig. 4</p> <p>H = 1000</p>	<p>Interpretation based on <math>\zeta</math> spectra, see Fig.7</p> <p>  (D)   (A)                 </p> <p>H = 10</p>	<p>Interpretation based on <math>\zeta</math> spectra, see Fig. 6</p> <p>  (C)   (B)                 </p> <p>H = 1000</p>
 <p><math>\alpha_1 = .5</math></p>	<p>(i) Repetitive buckle folds initiate almost simultaneously throughout multilayer.</p> <p> <math>\mathcal{L}_d/h = 70</math>  <math>\mathcal{L}_d/H = .07</math>  <math>\epsilon_{crit}(\theta_d) \approx .10</math> </p>	<p>(xi) Isolated buckle folds initiate.</p> <p> <math>\mathcal{L}_d/h = 6.1</math>  <math>\mathcal{L}_d/H = .61</math>  <math>\epsilon_{crit}(\theta_d) \approx .16</math> </p>	<p>(vi) Isolated buckle fold structures with a strong wavelength dependence on existing imperfections.</p> <p><math>\epsilon_{crit}(\theta_d) \approx .30</math></p>
 <p><math>\alpha_1 = .1</math></p>	<p>(iv) Theory N/A. Single layer buckling unlikely, brittle failure probable in both (A) and (D).</p> <p><math>\epsilon_{crit}(\theta_d) \approx .28</math></p>		<p>(ix) Theory N/A. Brittle shear fractures or localised kinking. Weak preference for <math>\theta_d \approx 32^\circ</math>.</p> <p><math>\epsilon_{crit}(\theta_d) \approx .42</math></p>
 <p><math>\alpha_1 = .02</math></p>	<p>(v) Theory N/A. Failure within very low amplitude single layer buckles. Fractures may propagate into weaker layers.</p> <p><math>\epsilon_{crit}(\theta_d) \approx .60</math></p>		<p>(x) Theory N/A. Brittle shear fractures or localised kinking. Strong preference for conjugate bands at <math>\theta_d \approx 35^\circ</math>.</p> <p><math>\epsilon_{crit}(\theta_d) \approx .47</math></p>
 <p><math>\alpha_1 = .9</math></p>	<p>(ii) Localized zones of kink-buckle hybrid structures Strong dependence on existing imperfections.</p> <p><math>\epsilon_{crit}(\theta_d) \approx .26</math></p>	<p>(xii) Localized zones at <math>\theta_d \approx 28^\circ</math> becoming rapidly indistinguishable from concentric-like folds due to high bending resistance.</p> <p><math>\epsilon_{crit}(\theta_d) \approx .32</math></p>	<p>(vii) Kink-buckle hybrid structures. Folding with strong dependence of wavelength on imperfections.</p> <p><math>\epsilon_{crit}(\theta_d) \approx .45</math></p>
 <p><math>\alpha_1 = .98</math></p>	<p>(iii) Localized zones of kinking. Strong preference for conjugate kinking at <math>\theta \approx 33^\circ</math>.</p> <p><math>\epsilon_{crit}(\theta_d) \approx .40</math></p>	<p>(xiii) Localized zones of kinking initiate at <math>\theta_d \approx 34^\circ</math>. The rapid propagation would establish a train of concentric-like folds.</p> <p><math>\epsilon_{crit}(\theta_d) \approx .43</math></p>	<p>(viii) As for multilayer (vii).</p> <p><math>\epsilon_{crit}(\theta_d) \approx .65</math></p>

Fig. 9. A prediction of the embryonic form of geological structures that develop at the inception of instability. Several idealised multilayers with geologically meaningful material properties and geometric constitution are considered. These predictions assume that structures will initiate at significant imperfections at a bulk strain below the critical value for the perfect multilayer ( $\epsilon = \epsilon_{crit}(\theta_d)$ ). The precise predictions are based on the  $\zeta$ -spectra for  $\epsilon = 0.1$  the value of strain (fixed for the sake of discussion) for which it is assumed that interlayer slip is triggered at an imperfection. The stress state in these multilayers described by their  $\zeta$ -spectra (i.e. in terms of potential instability to heterogeneous simple shear in different orientations) just prior to the triggering of the imperfection, is taken to be the overriding factor guiding the initial propagation direction and form of the growing structure(s). It is also assumed that the ultimate strength of both materials is not exceeded at strains below  $\epsilon = 0.1$ .  $\mathcal{L}_d/h$  is the dominant wavelength to average layer thickness ratio.



A value of  $R$  significantly greater than 1 occurs in the first type of multilayer. It signifies that the internal buckling pattern can describe the displacement pattern at the embryonic stage for instability developing at the critical strain  $\epsilon_{\text{crit}}(\theta_d)$ . In one example shown in Fig. 9, instability is predicted at a relatively low strain ( $\epsilon_{\text{crit}}(\theta_d) = 0.1$ ). It is probable that a pervasive and quite regular buckling pattern will develop for this multilayer by propagation and reflection, if loss of cohesion between layers is retarded until strains of  $\epsilon = 0.1$ .

A value of  $R$  significantly less than 1 indicates that heterogeneous simple shear is localized and displacement and displacement gradients cannot be defined along the characteristic directions. This is typical of the second type of multilayer. The two structures that are known from experiments to propagate along directions oblique to the compression direction are shear fractures (faults) and kink bands. Which of these two structures is likely to develop depends on the value of  $\epsilon_{\text{crit}}(\theta_d)$  and whether there is a large or small number of layers in the confined multilayer. If  $\epsilon_{\text{crit}}(\theta_d)$  is large (e.g.  $>0.3$ ) and  $H$  is low (e.g.  $\approx 10$ ); it is likely that faulting will occur before flexing of layers develops sufficiently to encourage kinking.

Conjugate kink bands (tabular domains with boundaries separating rotated foliated or laminated elements inside the domain from relatively unrotated ones outside the domain) which become typically angular as finite geological structures, probably begin as embryonic structures with their axial planes oblique to the layering. The deformation local to the domain involves an initial flexing which the theory predicts will occur provided there exists a significant intrinsic anisotropy. According to Johnson (1977, Chapter 6) the bending resistance fixes the approximate width of the kink band or domain. This further supports the general proposition, here, that kink bands are the finite expression of combined elements of both intrinsic anisotropy that favours buckling instability and nonlinear material properties that will favour the localization of deformation for conditions where yielding approaches rapidly. The suggestion in Fig. 9 that regular repetitions of thin seams of incompetent material, such as are found in phyllites and foliated low-grade metamorphic rocks, are highly susceptible to kinking in shallow deformation environments, is generally supported by observations in the field.

Let us consider briefly how certain multilayer structures will be formed by viscous deformation processes, before discussing the proposed classification shown in Fig. 10.

#### *Viscous deformation*

Due to the correspondence principle (Biot 1965), an extension of the results of the power-law elastic instability analysis of confined multilayers to power-law viscous multilayers is, under certain restrictions, relatively straightforward.

A power-law model for flow, similar to the power-law elastic model used in this paper, may be expressed in the

form of the Weertman (1968) equation for simple shear at constant temperature. In pure shear it may be written as  $\dot{\epsilon} = (\tau/K)^{n_v}$  or  $\tau = K\dot{\epsilon}^{m_v}$  where the well known stress exponent  $n_v = 1/m_v$ ,  $\dot{\epsilon}$  is the direct strain-rate,  $\tau$  is the shear stress (introducing a factor of  $\frac{1}{2}$  when compared with the elastic model) and  $K$  and  $m_v$  are the material constants analogous to  $k$  and  $m$  in the elastic model. A viscous power-law multilayer analysis for internal instability (Latham 1983) was interpreted using an amplification-rate spectrum (analogous to the  $\zeta$ -spectrum). The relative growth rates of S-banded perturbations (Cobbold 1977a,b) associated with different characteristic directions from  $0$  to  $90^\circ$  were investigated for different multilayer configurations.

Spectra generated from both elastic and viscous models (Latham 1983) prompt the conclusion that the results which are summarized in Fig. 10 are broadly applicable to both models.

### DISCUSSION—INTRODUCING A CLASSIFICATION OF STRUCTURE GENESIS

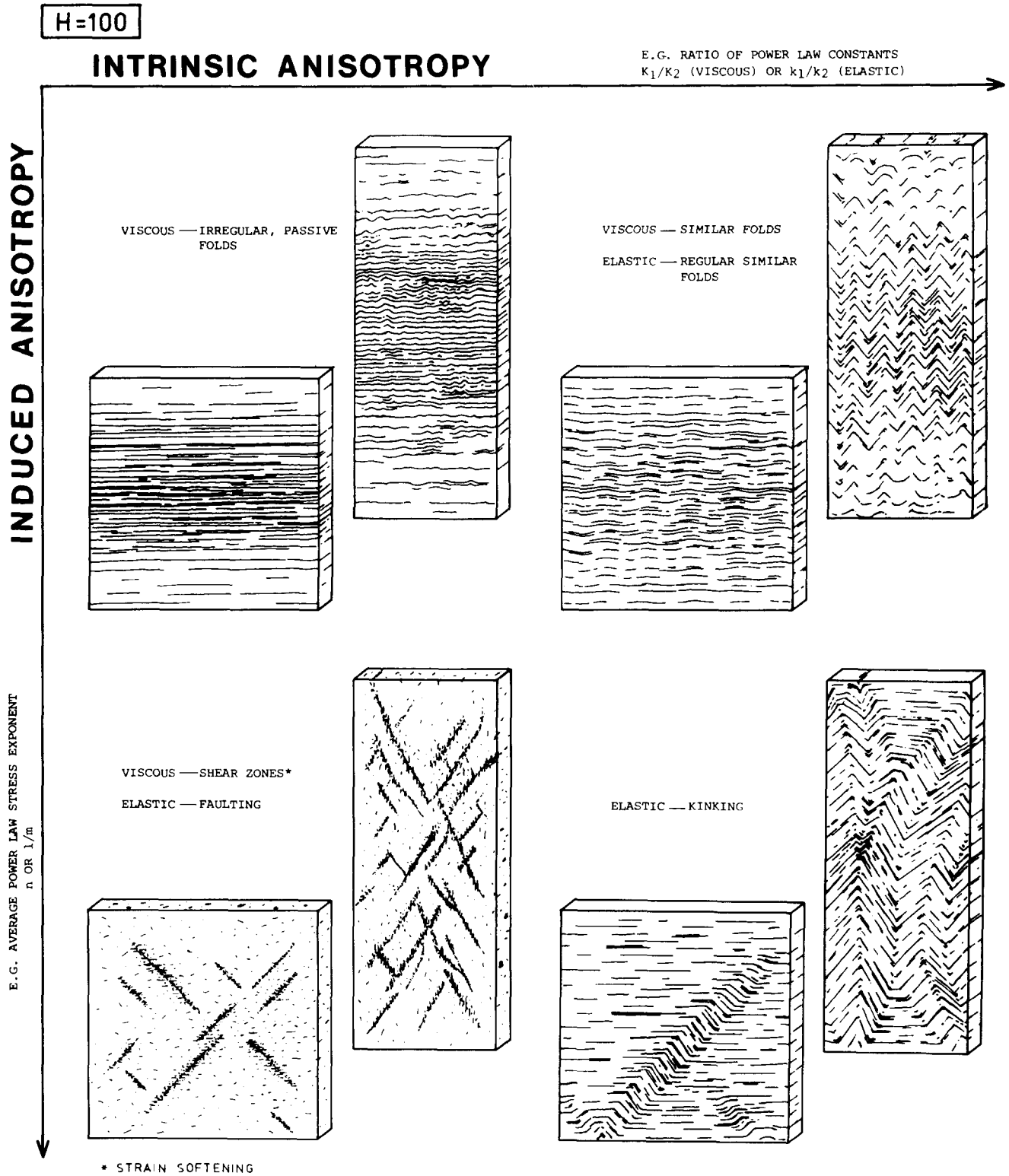
The results of this paper and its companion (Latham 1985) may be illustrated in the form of a classification of structure genesis (Fig. 10). The two different sources of incremental anisotropy, discussed in the companion paper, intrinsic and induced anisotropy, are shown as axes. They define an incremental anisotropy field on to which the structures arising from internal instability can be arranged according to the relative contributions of the two sources of anisotropy at the point of instability.

The rectangular sections represent a further (47%) finite plane strain shortening superimposed on the initial states. The structures that are likely to evolve from these initial instability types have been sketched on the basis of well documented experimental and theoretical evidence where mass transfer processes are negligible.

#### *Passive folding—top left, Fig. 10*

One obvious result of the internal instability analysis (Latham 1985) is that an incremental anisotropy is necessary for internal instability. There can be no internal instability in an intrinsically isotropic or poorly foliated material until a sufficient period of uniform loading has produced a high induced anisotropy. There is therefore no structure from the upper crustal deformation environment (i.e. where time-independent deformation mechanisms may be assumed to predominate) that can be allocated to this quarter of the field.

A theoretical analysis of the viscous multilayer with parameters corresponding to this particular corner of Fig. 10, i.e. low average  $n_v$  and low  $K_1/K_2$  produces an amplification-rate spectrum which predicts that selectivity of the fastest growing shear perturbation is very poor. In these inactive multilayers, the passive flattening deformation will tend to swamp the active growth of perturbations and so the finite fold disturbances acquire an irregular wavelength reflecting initial irregularities,



eventually with axial planes rotated subparallel to the extension direction. Folds of similar style found in the metamorphosed feldspathic sandstones (Moine Series) near Monar, Scotland were probably formed by this mechanism involving a very large shortening. The lack of discernible structures in the square section in Fig. 10 indicates the relative stability of this configuration. The additional finite pure shear shows only the predicted viscous response, i.e. irregular passive folding and an elastic-plastic response is not shown for reasons given above.

*Oblique localized shearing—bottom left, Fig. 10*

The detailed analysis of faulting in porous sandstones presented by Aydin & Johnson (1983) will now be briefly discussed as it is extremely pertinent to the mechanism of faulting assumed in the investigation of this paper. Armed with a theory of localization of deformation within homogeneous materials (Rudnicki & Rice 1975) and a theory of runaway instability (Rudnicki 1977), Aydin & Johnson presented an explanation for the development of various faults that were observed in the Entrada and Navajo sandstones. These were of three different types: deformation bands, zones of deformation bands and slip surfaces within deformation bands. The constitutive behaviour of the porous rock assumed in the analyses is a sophisticated strain-hardening Coulomb model allowing for friction, cohesion, dilatancy and elasticity all to be functions of strain.

The critical condition for which planar banding can begin is satisfied under certain combinations of the strain dependent moduli. The reader concerned specifically with the application of shear banding criteria to faulting mechanisms is referred to Aydin & Johnson's examination of these moduli.

On a historical note about which there appears to be some confusion, it is worth pointing out that this general and three-dimensional condition or criterion for localization signalled by the inception of banding and given by Rudnicki & Rice (1975) has been known in the solid mechanics disciplines for some time. It is equivalent to the condition given by Hill (1962) for a "stationary discontinuity". An important link in the history of the use of this criterion was revealed by Hill & Hutchinson (1975 appendix (ii)) who showed that Hill's (1962) stationary discontinuity condition, when expressed in a form specifically for plane strain and incompressible deformation, becomes identical to that for Biot's internal instability of the second kind. These developments firmly indicate that the condition for second-kind end-member behaviour referred to in this paper, will represent a shear banding instability albeit a specialized case.

Returning now to the  $\zeta$ -spectrum of the elastic analysis, the shear-band network in the figure seems a highly plausible physical interpretation. In contrast, the amplification-rate spectrum of the viscous fluid analysis shows no peaks about the 45° orientation and it is generally agreed that deformation cannot localize into shear bands within a strain-rate hardening ( $n_v > 1$ )

nonlinear viscous rock unless there are in addition flow softening mechanisms which may become operative. (A likely candidate in high temperature pressure conditions would be dynamic recrystallization by grain boundary migration; see Poirier (1980) for a fuller discussion of flow softening mechanisms.)

It is often assumed that rocks exhibiting a highly nonlinear stress/strain-rate dependence in flow (e.g.  $n_v > 3-5$ ) are more prone to flow softening, where the stress drops for an additional increment of strain or an increase in strain-rate, than rocks with more linear fluid properties. It is perhaps not unreasonable therefore to consider a ductile shear-zone network as the induced anisotropy end member structure preserved from deeper deformation environments where time-dependent (i.e. viscous) nonlinear flow has been accompanied by flow softening.

The sketch in Fig. 10 is of structures produced by localized shearing, either discrete shear fractures or shear bands. These structures are common in natural examples of nominally isotropic rocks deformed in shallow and deep crustal environments. For example, shear fractures are common in massive limestones and sandstones and both shear fractures and shear zones are found in many igneous rocks, particularly granites.

*Active internal buckling—top right, Fig. 10*

For both elastic and viscous applications of the multilayer analysis, the structures predicted for the intrinsic anisotropy end member result from active selection of directions (sub-normal to the compression direction) for the propagation of heterogeneous simple shear. The propagating disturbance, if fast enough, will reflect off the multilayer boundaries and interfere (Cobbold 1976a) producing an internal buckling when the simple shear is sinusoidal as will usually be the case during the early flexing of planar elements or layers. A more regular periodicity in the folding is expected in folds initiating during elastic loading as the propagation rates will be faster.

Typically, if a wave train of folds is established at low amplitudes, these folds should display very little layer-parallel shortening with chevron profiles at moderate limb-dips (e.g. see Cobbold 1976b). However, where pressure-solution mechanisms are important in shaping folds, most demonstrably on the small scale, regular packets of more rounded folds of the type associated with crenulation cleavage can also develop in rocks with a high intrinsic anisotropy.

*Kinking—bottom right, Fig. 10*

In the nonlinear elastic analysis of the previous section (e.g. Fig. 8) the interpretation of  $\zeta$ -spectra for certain selections of physical and geometric multilayer parameters ( $k_1/k_2$ ,  $m_1$ ,  $m_2$ ,  $\alpha_1$  and  $H$ ) lead to the suggestion that kink-bands would be the most likely structures to initiate when both intrinsic anisotropy and induced anisotropy contribute in favourable proportions to the average

continuum properties at instability. Kinking, it was suggested by Johnson (1977), involves both flexing and yielding. The discussion in this paper would certainly support this view.

Honea & Johnson (1976) presented a mechanical analysis of conditions which favour kinking in preference to amplification of internal buckles in uniform multilayers under layer parallel compression. A high "average shear modulus" relative to "contact strength" between layers and a high initial slope of irregularities were found to favour kink folding. Although their analysis which considers the elastic stability of a single plate under certain boundary stresses differs considerably from the continuum approach used here, their conclusion that high intrinsic anisotropy will favour the amplification of internal buckles more than kinking is in agreement with the findings of the continuum analysis presented in this paper. Presumably, the role played by the highly nonlinear material property of "contact strength" between laminae in Honea and Johnson's analysis is in part represented by the role played by the nonlinear material properties that are connected with induced anisotropy and yielding and are accounted for in the continuum analysis. This is the most likely reason for the encouraging agreement between the differing analyses.

On the subject of kinking mechanisms, observations of kinking in Honea & Johnson's (1976) displacement controlled model experiments using strips of rubber in frictional contact are particularly revealing but should be interpreted carefully because of the instantaneously recoverable strain energy in the rubber.

In order that conjugate kink-bands should appear as isolated structures within unrotated layering, it is necessary that the propagation from an isolated imperfection is sufficiently fast relative to amplification so that no significant disruption of layering by amplification of other layer perturbations can have occurred (see the discussion by Cobbold 1976a). This is one reason why elastic strain energy should be a major consideration in analyses of kinking mechanisms as should the post-bifurcation deformation which may involve elastic unloading.

Summers (1979) produced a finite deformation rotation band analysis for an intrinsically anisotropic linear viscous continuum. Although his idea that the kinking mechanism is fundamentally related to rotational instability is attractive, for kinks to develop in foliated layered rocks behaving as though they were anisotropic viscous continua seems unlikely. It is difficult to imagine a volume of rock extensive enough to exhibit kink bands in which the anisotropy remains sufficiently planar while in a purely strain-rate dependent deformation environment. If however the deformation environment allows the rocks to behave as elastic-viscous or elastic-plastic materials, then the viscous or plastic deformation can occur more locally perhaps concentrating within interbeds or laminae interfaces and zones of maximum bending while the surrounding layering remains planar due to its elastic rigidity. The efficiency with which the energy from the surrounding layering can be channeled into propagating a localized kink-band is probably a crucial

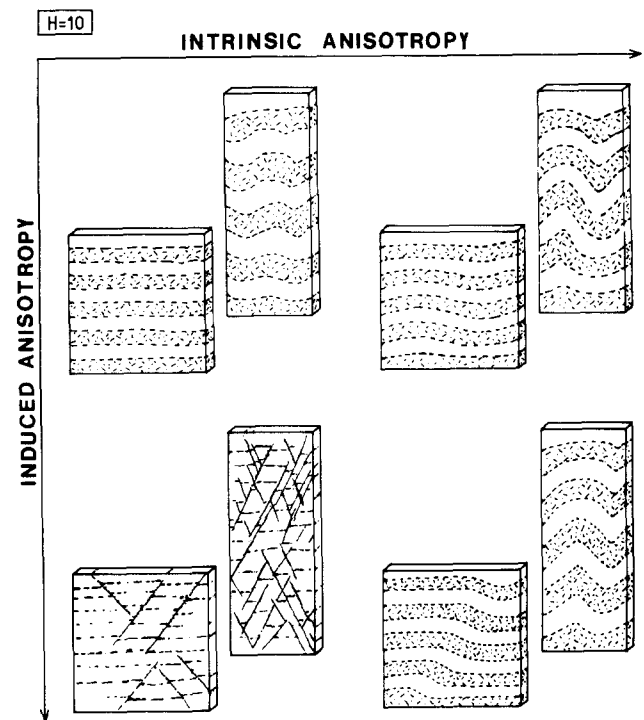


Fig. 11. Summary diagram of structures as in Fig. 10 but where the multilayer has a high resistance to bending, having few layers ( $H = 10$ ).

factor. Within a developing kink-band, deformation may be primarily by a viscous controlled rotation resulting from a high intrinsic anisotropy which is only operative inside the band.

#### *Effect of bending resistance*

The most direct influence that an increase in bending resistance will have has been investigated by considering a confined multilayer with very few layers. With  $H = 10$ , the alternative set of block diagrams (Fig. 11) was sketched to indicate some of the modifications of the extreme types of instability that can be expected. The figure shows how the present theory helps to explain why buckle and conjugate kink bands are often particularly indistinguishable for the case where there are only a few layers in the confined multilayer. This is because the dominant characteristics associated with internal buckling are shifted to more oblique angles to the extension direction, i.e. nearer to the typical kink band orientations, when the resistance to bending is higher.

#### *Concluding remarks*

The block diagrams (Figs. 10 and 11) indicate two important mechanical principles. A high intrinsic anisotropy will be associated with ordered structures of greater regularity. High induced anisotropy is associated with localized deformation.

From the present understanding of the material properties of rocks in the Earth's crust and how these may contribute to average anisotropic properties, it seems reasonable from mechanical considerations to expect that most natural structures that initiate out of a uniform

state of 'layer' parallel compression, may be understood to be hybrids of the four extreme cases: passive amplification of initial irregularities, internal buckling, oblique localized shearing into bands and kinking, illustrated in Fig. 10. The main purpose of this somewhat oversimplified classification of structure genesis is to show the underlying mechanical relationships that exist between these apparently diverse geological structures.

*Acknowledgements*—Part of this work was carried out during the tenure of a N.E.R.C. studentship which is gratefully acknowledged. Dr. J. W. Cosgrove's comments have helped considerably with the presentation of this work.

## REFERENCES

- Aydin, A. & Johnson, A. M. 1983. Analysis of faulting in porous sandstones. *J. Struct. Geol.* **5**, 19–31.
- Biot, M. A. 1964. Theory of internal buckling of a confined multilayered structure. *Bull. geol. Soc. Am.* **75**, 563–568.
- Biot, M. A. 1965. *Mechanics of Incremental Deformations*. Wiley, New York.
- Biot, M. A. 1965a. Theory of similar folding of the first and second kind. *Bull. geol. Soc. Am.* **76**, 251–258.
- Biot, M. A. 1965b. Internal instability of anisotropic viscous and viscoelastic media under initial stress. *J. Franklin Inst.* **279**, 65–82.
- Biot, M. A. 1965c. Further development of the theory of internal buckling of multilayers. *Bull. geol. Soc. Am.* **76**, 833–840.
- Biot, M. A. 1967. Rheological stability with couple stresses and its application to geological folding. *Proc. R. Soc.* **A298**, 402–423.
- Cobbold, P. R. 1976a. Fold shapes as functions of progressive strains. *Phil. Trans. R. Soc.* **A283**, 129–138.
- Cobbold, P. R. 1976b. Mechanical effects of anisotropy during large finite deformations. *Bull. Soc. geol. Fr.* **18**, 1497–1510.
- Cobbold, P. R. 1977a. Description and origin of banded deformation structures—I. Regional strain, local perturbations and deformation bands. *Can. J. Earth Sci.* **14**, 1721–1731.
- Cobbold, P. R. 1977b. Description and origin of banded deformation structures—II. Rheology and the growth of banded perturbations. *Can. J. Earth Sci.* **14**, 2510–2523.
- Cobbold, P. R., Cosgrove, J. W. & Summers, J. M. 1971. Development of internal structures in deformed anisotropic rocks. *Tectonophysics* **12**, 25–53.
- Hill, R. 1962. Acceleration waves in solids. *J. Mech. Phys. Solids* **10**, 1–16.
- Hill, R. & Hutchinson, J. W. 1975. Bifurcation phenomena in the plane tension test. *J. Mech. Phys. Solids* **23**, 239–264.
- Honea, E. & Johnson, A. M. 1976. A theory of concentric, kink and sinusoidal folding and of monoclinical flexing of compressible elastic multilayers—III. Transition from sinusoidal to concentric-like to chevron folds. *Tectonophysics* **27**, 1–38.
- Hutchinson, J. W. & Tvergaard, V. 1981. Shear band formation in plane strain. *Int. J. Solids Structures* **17**, 451–470.
- Johnson, A. M. 1977. *Styles of Folding*. Elsevier, Amsterdam.
- Johnson, A. M. 1980. Folding and faulting of strain-hardening sedimentary rocks. *Tectonophysics* **62**, 251–278.
- Latham, J-P. 1983. The influence of mechanical anisotropy on the development of geological structures. Unpublished Ph.D. thesis, University of London.
- Latham, J-P. 1985. The influence of nonlinear material properties and bending resistance upon the development of internal structures. *J. Struct. Geol.* **7**, 225–236.
- Poirier, J. P. 1980. Shear localisation and shear instability in materials in the ductile field. *J. Struct. Geol.* **2**, 135–142.
- Price, N. J. 1975. Fluids in the crust of the earth. *Sci. Prog., Lond.* **62**, 59–87.
- Rice, J. R. 1976. The localisation of plastic deformation. *Proc. 14th Int. Congr. Theor. Appl. Mech.* (edited by Koiter, W. T.). North Holland, Amsterdam, 207–220.
- Rudnicki, J. W. 1977. The inception of faulting in a rockmass with a weakened zone. *J. geophys. Res.* **82**, 844–854.
- Rudnicki, J. W. & Rice, J. R. 1975. Conditions for the localisation of deformation in pressure-sensitive dilatant materials. *J. Mech. Phys. Solids* **23**, 371–394.
- Summers, J. M. 1979. An experimental and theoretical investigation of multilayer fold development. Unpublished Ph.D. thesis, University of London.
- Weertman, J. 1968. Dislocation climb theory of steady-state creep. *Am. Soc. Metals Trans.* **61**, 681–694.